Published in final edited form as:
J Dent Res. 2009 April ; 88(4): 318–322. doi:10.1177/0022034509334749.

Synergistic Roles of Amelogenin and Ameloblastin

J. Hatakeyama[1], **S. Fukumoto**[2], **T. Nakamura**[2], **N. Haruyama**[1], **S. Suzuki**[1], **Y. Hatakeyama**[3], **L. Shum**[3], **C. W. Gibson**[4], **Y. Yamada**[2], and **A. B. Kulkarni**[1,+]

[1] Functional Genomics Section, Laboratory of Cell and Developmental Biology, National Institutes of Health, Bethesda, MD 20892, USA

[2] Molecular Biology Section, Laboratory of Cell and Developmental Biology, National Institute of Dental and Craniofacial Research, National Institutes of Health, Bethesda, MD 20892, USA

[3] Cartilage Biology and Orthopedics Branch, National Institute of Arthritis and Musculoskeletal and Skin Diseases, National Institutes of Health, Bethesda, MD 20892, USA

[4] Department of Anatomy and Cell Biology, University of Pennsylvania School of Dental Medicine, Philadelphia, PA, 19104, USA

Abstract

Amelogenin and ameloblastin, the major enamel matrix proteins, are important for enamel mineralization. In order to identify their synergistic roles in enamel development, we generated *Amel* $X^{-/-}$/*Ambn*$^{-/-}$ mice. These mice showed additional enamel defects as compared to *Amel* $X^{-/-}$ or *Ambn*$^{-/-}$ mice. In 7 day old *Amel* $X^{-/-}$/*Ambn*$^{-/-}$ mice, the ameloblast layer was not only irregular and detached from the enamel surface like in *Ambn*$^{-/-}$, but additionally the enamel width was significantly reduced in the double null mice as compared to *Amel* $X^{-/-}$ or *Ambn*$^{-/-}$ mice. Proteomic analysis of the double null teeth revealed increased level of RhoGDI (Arhgdia), a Rho family-specific guanine nucleotide dissociation inhibitor, which is involved in important cellular processes, such as cell attachment. Both *Amel* $X^{-/-}$/*Ambn*$^{-/-}$ mice and *Ambn*$^{-/-}$ mice displayed positive staining with RhoGDI antibody in the irregularly-shaped ameloblasts detached from the matrix. Ameloblastin-regulated expression of RhoGDI suggests that Rho-mediated signaling pathway might play a role in enamel formation.

Keywords

enamel; amelogenin; ameloblastin; knockout mice; RhoGDI (Arhgdia)

INTRODUCTIONS

Dental enamel is the most highly mineralized tissue in the body, and is formed as a result of mineralization of enamel matrices secreted by ameloblasts. Ameloblasts secrete several enamel matrix proteins, such as amelogenins, ameloblastin, and enamelin. These enamel matrix proteins are processed and degraded by proteases such as MMP20 and KLK4 during the enamel mineralization (Bartlett *et al*., 1996; Simmer *et al*., 1998). The highly orchestrated secretion of enamel matrix proteins and their proper degradation are critical for the normal enamel formation.

+Corresponding author: Ashok Kulkarni, PhD, Functional Genomics Section, LCDB, NIDCR, NIH, 30 Convent Dr., MSC 4395, Bethesda, MD, USA 20892, Phone: 301-435-2887, FAX: 301-435-2888, ak40m@nih.gov.

The amelogenin proteins are highly conserved across species, and constitute 90% of the enamel organic matrix. Based on the results from our study of *Amel X*$^{-/-}$ mice, amelogenins play an important role in enamel biomineralization (Gibson *et al*., 2001, Hatakeyama *et al.*, 2003). In the *Amel X*$^{-/-}$ mice, ameloblast differentiation was relatively normal but an abnormally thin enamel layer was formed (Gibson *et al*., 2001 and 2005). It was concluded that amelogenins are essential for the well-organized hydroxyapatite prism formation and elongation during enamel development and for producing the normal enamel thickness but not for initiation of enamel formation. Our recent studies have demonstrated that transgenic mice that express M180, which is the most abundant amelogenin isoform, was able to significantly rescue the enamel defects of amelogenin null mice (Yong *et al*., 2008). Self-assembly of amelogenin proteins into nanospheres has been recognized as a key factor in controlling the orientation and elongated growth of crystals during the mineralizing process in enamel (Du *et al.,* 2005). Transgenic mice that express an amelogenin protein with a mutated N or C terminus showed that N-terminal domain of amelogenin might be involved with the formation of nanospheres (Paine *et al*., 2003a), whereas the C-terminal region could contribute to stability and homogeneity in size of nanospheres, preventing mineral crystal fusion to form larger structures prematurely (Moradian-Oldak *et al*., 2005 and 2006). In addition, we have recently reported its function for osteoclast differentiation in periodontal ligament tissue (Hatakeyama *et al*., 2006).

Ameloblastin, also known as amelin or sheathlin, is an enamel-specific glycoprotein, which is the most abundant non-amelogenin enamel matrix protein (Cerný *et al*., 1996; Krebsbach *et al*., 1996; Fong *et al*., 1998), and serves as a cell adhesion molecule for ameloblasts but not for dental epithelial cells (Fukumoto *et al*., 2004 and 2005). Ameloblastin expression in ameloblasts peaks at the secretory stage and diminishes at the maturation stage. Transgenic mice overexpressing ameloblastin in ameloblasts have impaired enamel structures, suggesting the importance of normal levels of ameloblastin in enamel formation (Paine *et al*., 2003b). Furthermore, in *Ambn*$^{-/-}$ mice, the dental epithelium differentiates into enamel-secreting ameloblasts, but the cells detach from the matrix surface at the secretory stage and lose polarity. In ameloblasts of *Ambn*$^{-/-}$ teeth, the expression of amelogenins is reduced to about 20% of that of *Ambn*$^{+/+}$ teeth, while other enamel matrix proteins are expressed at nearly normal levels (Fukumoto *et al*., 2004). These results suggested that ameloblastin is essential in maintaining normal ameloblast differentiation and attachment to the enamel matrix. Thus, the cellular functions of amelogenin and ameloblastin are apparently distinct, and in this paper we report potential synergistic functions of these two enamel proteins.

MATERIAL AND METHODS

Amel X$^{-/-}$/Ambn$^{-/-}$ mice

Targeted disruption of amelogenin (*Amel X)* and ameloblastin (*Ambn*) genes was described previously (Gibson *et al*., 2001; Fukumoto *et al*., 2004). *Amel X*$^{-/-}$ mice were mated with *Ambn*$^{-/-}$ mice to generate double heterozygous mice, which were interbred to generate *Amel X*$^{-/-}$/*Ambn*$^{-/-}$ mice. Detailed information on generation and genotyping is described in the Supplemental Material. Mutant mice were initially analyzed in the C57BL/6 × 129/SvEv mixed genetic background and later in enriched C57BL/6 background by backcrossing four times with C57BL/6 mice. Standard NIH guidelines were followed to house, feed and breed the mice. These studies were carried out with the approval of the NIDCR Animal Care and Use Committee.

Scanning Electron Microscopic (SEM) Analyses of Incisors and Molars

Incisors and molars from wild type and mutant mice were coated with gold and photographed using scanning electron microscopy at 20 kV (Jeol JSM T330A, Jeol, Inc., Peabody, MA), and energy dispersive spectroscopy (Kevex X-ray, Scotts Valley, CA).

To observe the enamel crystals, the specimens were embedded in epoxy resin, cut with an ISOMET low speed saw (Buehler, Lake Bluff, IL), and then treated with 40% phosphoric acid for 10 s and 10% sodium hypochlorite for 30 s, and then coated with gold.

Preparation of Tissue Sections and Immunohistochemistry

Postnatal day 1 (P1) and P7 mouse skulls were dissected from and fixed with 4 % paraformaldehyde in phosphate-buffered saline (PBS) for 16 hours at 4°C. Tissues were decalcified with 250 mM EDTA/PBS and embedded in paraffin for paraffin sections or in OCT compound (Sakura Finetechnical Co., Torrance, CA) for frozen sectioning. Frozen sections were cut at 8 μm on a cryostat (2800 Frigocut, Leica Inc. Wetziar, Germany). Paraffin sections were cut at 5 μm on a microtome (RM2155, Leica Inc.). For the detailed morphological analysis, sections were stained with hematoxylin and eosine Y (Sigma, St. Louis, MO). Frozen sections were immunostained for RhoGDI using goat polyclonal antibodies against mouse RhoGDI (Santa Cruz Biotechnology, Santa Cruz, CA) overnight at 4°C at a dilution of 1:100. After washing with PBS, the sections were incubated with peroxidase-conjugated mouse antibodies against goat IgG (Vector Laboratories, Burlingame, CA), treated with diaminobenzidine substrate and counterstained with hematoxylin for light microscopy. For control, frozen sections were incubated only with secondary antibody.

RESULTS

Defective enamel formation in Amel X$^{-/-}$/Ambn$^{-/-}$ mice

SEM analysis of incisors revealed a hypoplastic enamel and a lack of prism pattern in *Amel X*$^{-/-}$, *Ambn*$^{-/-}$ and *Amel X*$^{-/-}$/*Ambn*$^{-/-}$ mice that is the hallmark of organized mineral crystals in normal enamel (Fig. 1A–D). Enamel width was much thinner in *Amel X*$^{-/-}$/*Ambn*$^{-/-}$ mice as compared to *Amel X*$^{-/-}$ and *Ambn*$^{-/-}$ mice. As in *Ambn*$^{-/-}$ mice flat plate-like structures extended perpendicular from the enamel surface to the dentin enamel junction in *Amel X*$^{-/-}$/*Ambn*$^{-/-}$ mice (Fig. 1C and D). The enamel surfaces appeared cobbled in both *Amel X*$^{-/-}$ (Fig. 1J) and Ambn$^{-/-}$(Fig. 1K) mice. However in *Amel X*$^{-/-}$/*Ambn*$^{-/-}$ mice, the molar surfaces appeared less cobbled than in *Amel X*$^{-/-}$ and *Ambn*$^{-/-}$ mice (Fig. 1L). Elemental analysis indicated that the composition was similar to that of hydroxyapatite, indicating a normal formation of mineral in the absence of the amelogenin and ameloblastin proteins. Ca/P molar ratio was also not significantly different in the teeth of all null mice and the WT controls (almost 1.5, data not shown).

Unlike Ambn$^{-/-}$ ameloblasts, Amel X$^{-/-}$/Ambn$^{-/-}$ ameloblasts do not develop calcified nodules

In early stages of molar development up to P1, no differences were observed in either shape or size of the tooth-buds of WT, *Amel X*$^{-/-}$, *Ambn*$^{-/-}$, and *Amel X*$^{-/-}$/*Ambn*$^{-/-}$ mice (Fig. 2A–D). At P1, dentin formation of molars had begun and dental epithelium had started to elongate and polarize with the apical nuclear localization in all of these mice (Fig. 2E–H). Thus, cellular organization of ameloblasts and odontoblasts was similar in these mice at the presecretory stage. However, at P3, ameloblasts of *Ambn*$^{-/-}$ and *Amel X*$^{-/-}$/*Ambn*$^{-/-}$ mice started to detach from the matrix layer and lost the cell polarity with the centralized nuclear localization (Fig. 2K and L), whereas normal ameloblasts were polarized, elongated, and formed an enamel matrix in WT and *Amel X*$^{-/-}$ mice (Fig. 2I and J). At P7, *Ambn*$^{-/-}$ and *Amel X*$^{-/-}$/*Ambn*$^{-/-}$

ameloblasts completely lost their polarity (short and round shape) and accumulated to form a multilayered structure (Fig. 2O and P, arrow head), in contrast to the single layer of WT and *Amel X*$^{-/-}$ ameloblasts (Fig. 2M and N). Interestingly, *Ambn*$^{-/-}$ ameloblasts contained calcified nodules (Fig. 2O, arrow), but *Amel X*$^{-/-}$/*Ambn*$^{-/-}$ cells did not (Fig. 2P).

Increase RhoGDI expression in Amel X$^{-/-}$/Ambn$^{-/-}$ ameloblasts

As described in the Supplemental Material, we utilized proteomic analysis to identify 24 kDa-size protein, which was increased in *Amel X*$^{-/-}$/*Ambn*$^{-/-}$ ameloblasts. Using MALDI analysis we identified this protein as RhoGDI. For further analysis of RhoGDI expression pattern in developing of mouse molars, we carried out the immunohistochemical analysis. At P1, weak RhoGDI expression was observed in ameloblasts and odontoblasts of the WT, *Amel X*$^{-/-}$, *Ambn*$^{-/-}$, and *Amel X*$^{-/-}$/*Ambn*$^{-/-}$ mice (Fig. 3A–D). However, at P7, the ameloblasts of WT and *Amel X*$^{-/-}$ mice had no noticeable RhoGDI expression (Fig. 3E and F), whereas irregular-shaped ameloblasts in *Ambn*$^{-/-}$ and *Amel X*$^{-/-}$/*Ambn*$^{-/-}$ mice showed sustained expression of RhoGDI (Fig. 3G and H). Calcified nodules were also noticed adjacent to the irregular ameloblast layer in *Ambn*$^{-/-}$ mice (Fig. 3G, arrow) but not in *Amel X*$^{-/-}$/*Ambn*$^{-/-}$ mice. We also noted increased expression of RhoGDI in the lower first molars of the 7 day old *Amel X*$^{-/-}$/*Ambn*$^{-/-}$ mice by RT-PCR (Supplemental Fig. 3)

DISCUSSION

In order to delineate potential synergistic roles of amelogenins and ameloblastin, we analyzed teeth from the wild-type, *Amel X*$^{-/-}$, *Ambn*$^{-/-}$ and *Amel X*$^{-/-}$/*Ambn*$^{-/-}$ mice. Our analysis revealed that the *Amel X*$^{-/-}$/*Ambn*$^{-/-}$ mice displayed additional enamel defects. As compared to the *Amel X*$^{-/-}$ and *Ambn*$^{-/-}$ mice, enamel-width was markedly reduced in *Amel X*$^{-/-}$/*Ambn*$^{-/-}$ mice. Although ameloblast morphology was similar in *Ambn*$^{-/-}$ and *Amel X*$^{-/-}$/*Ambn*$^{-/-}$ mice, calcified nodules observed in *Ambn*$^{-/-}$ ameloblasts were absent in the double null ameloblasts. These additional defects in *Amel X*$^{-/-}$/*Ambn*$^{-/-}$ ameloblasts suggest a possible synergism in the cellular functions of amelogenins and ameloblastin.

Surprisingly, *Amel X*$^{-/-}$/*Ambn*$^{-/-}$ mice still showed a very thin layer of enamel in spite of the lack of two most abundant ECM proteins secreted by ameloblasts to form normal enamel. We found that enamelin is still expressed in the *Amel X*$^{-/-}$/*Ambn*$^{-/-}$ teeth (based on our RT-PCR analysis; data not shown). Enamelin gene (ENAM) has been also implicated in human amelogenesis imperfecta (Kim *et al*., 2005). *Enam*$^{-/-}$ mice did not from normal enamel because of the lack of a mineralization at the secretory surface of the ameloblasts (Hu *et al*., 2008). In addition, ENAM point mutation resulted in the phenotype resembling amelogenesis imperfecta (Masuya *et al*., 2005). Therefore, it is possible that enamelin might be involved in the enamel formation in the *Amel X*$^{-/-}$/*Ambn*$^{-/-}$ mice. In addition to enamelin, other ECM proteins might play a role in the enamel formation in these mice and their identification will require further studies. We had earlier reported that amelogenins are involved in osteoclast differentiation in PDL cells, and furthermore one can speculate its lack in the double null mice might contribute in some way in the formation of thinner enamel. Interestingly, SEM analysis of molars and incisors indicated smoother enamel in the *Amel X*$^{-/-}$/*Ambn*$^{-/-}$ mice as compared to *Ambn*$^{-/-}$ enamel. This phenotypic difference can be possibly attributed to the presence of irregular calcified nodules in *Ambn*$^{-/-}$ ameloblasts and one can speculate that these nodules are formed because of the residual amelogenin in these mice (Fukumoto *et al*., 2004).

Our proteomic studies identified that increased protein level of RhoGDI (Arhgdia) in *Amel X*$^{-/-}$/*Ambn*$^{-/-}$ teeth. RhoGDI, a Rho family-specific guanine nucleotide dissociation inhibitor, forms a tight complex with Rho GTPases and inactivates Rho GTPases functions as a cytosolic molecule. Reduced expression or inactivation of RhoGDIs releases Rho GTPases from the complex and translocates Rho GTPases into the membrane for activation of Rho signaling

pathways (Takai *et al*., 1995). Rho GTPases such as Rho, Rac, and Cdc42, are known to regulate assembly of filamentous actin (F-actin) and the organization of the actin cytoskeleton, and the regulation of gene transcription, cell cycle, microtubule dynamics, vesicle transport and numerous enzymatic activities. In the wild-type teeth, RhoGDI was expressed in undifferentiated dental epithelium, but its expression was down regulated in the secretory stage of ameloblasts. During the tooth development, protein expression of RhoGDI is not altered at the early stage in *Amel* $X^{-/-}$, *Ambn*$^{-/-}$ and *Amel* $X^{-/-}$/*Ambn*$^{-/-}$ ameloblasts. However, in later stages, when cells continue to proliferate and form multicellular layers in *Amel* $X^{-/-}$/*Ambn*$^{-/-}$ mice, RhoGDI expression is increased. The Rho signaling pathways in murine ameloblasts are known to induce F-actin product (Li *et al*., 2005). F-actin rich regions have been described, and these include Tomes' process, distal terminal webs, and distal ends of ruffled or smooth ended ameloblasts in the rat incisors (Nishikawa *et al*., 1986).

Interestingly, the human Amel X gene was shown to reside in a "nested" gene structure within intron 1 of the ARHGAP6 gene that encodes Rho GAP, which regulates RhoA activity (Prakash *et al*., 2005; Hall *et al*., 2000). In some cases, expression of nested and host genes are simultaneously up-regulated or down-regulated by common regulatory elements (Peters and Ross, 2001). It is possible that the expression of Amel X and ARHGAP6 genes might be regulated in similar way. Rho is recognized as a molecular switch (Hall *et al*., 2000), that normally cycles from the active GTP-bound form to the inactive GDP-bound form (Li *et al*., 2005), thereby regulating downstream events leading to changes in the cytoskeleton. It has been shown that Rac1 and Cdc42, down stream of Rho signaling, are regulators of cell spreading and formation of lamellipodia and filopodia (Clark *et al*., 1998, Hall *et al*., 1998), and cell polarization (Cau *et al*., 2005, Etienne-Manneville *et al*., 2002). Rac1 and Cdc42 regulate laminin-10/11-mediated cell spreading and filopodia formation of the dental epithelium (Fukumoto *et al*., 2006). Increased expression of RhoGDI in *Amel* $X^{-/-}$/*Ambn*$^{-/-}$ tooth might inhibit active Rho GTP, resulting in irregular ameloblast morphology.

In summary, our study suggests that the enamel matrix proteins such as amelogenins and ameloblastin are not only required for the formation of a proper matrix for well-orchestrated enamel biomineralization but also have synergistic cellular functions during enamel development.

Supplementary Material

Refer to Web version on PubMed Central for supplementary material.

Acknowledgments

We thank Drs. Aya Yamada and Yoko Kamasaki for generous help with SEM analysis, and Harry Grant for editorial assistance. This work was supported by the Division of Intramural Research of the National Institute of Dental and Craniofacial Research.

References

Bartlett JD, Simmer JP, Xue J, Margolis HC, Moreno EC. Molecular cloning and mRNA tissue distribution of a novel matrix metalloproteinase isolated from porcine enamel organ. Gene 1996;183:123–128. [PubMed: 8996096]

Cau J, Hall A. Cdc42 controls the polarity of the actin and microtubule cytoskeletons through two distinct signal transduction pathways. J Cell Sci 2005;118:2579–2587. [PubMed: 15928049]

Cerný R, Slaby I, Hammarström L, Wurtz T. A novel gene expressed in rat ameloblasts codes for proteins with cell binding domains. J Bone Miner Res 1996;11(7):883–891. [PubMed: 8797107]

Clark EA, King WG, Brugge JS, Symons M, Hynes RO. Integrin-mediated signals regulated by members of the rho family of GTPases. J Cell Biol 1998;142:573–586. [PubMed: 9679153]

Du C, Falini G, Fermani S, Abbott C, Moradian-Oldak J. Supramolecular assembly of amelogenin nanospheres into birefringent microribbons. Science 2005;307:1450–1454. [PubMed: 15746422]

Etienne-Manneville S, Hall A, Rho GT. Pases in cell biology. Nature 2002;420:629–635. [PubMed: 12478284]

Fong CD, Cerny R, Hammarstrom L, Slaby I. Sequential expression of an amelin gene in mesenchymal and epithelial cells during odontogenesis in rats. Eur J Oral Sci 1998;106(Suppl 1):324–330. [PubMed: 9541243]

Fukumoto S, Kiba T, Hall B, Iehara N, Nakamura T, Longenecker G, et al. Ameloblastin is a cell adhesion molecule required for maintaining the differentiation state of ameloblasts. J Cell Biol 2004;167:973–983. [PubMed: 15583034]

Fukumoto S, Yamada A, Nonaka K, Yamada Y. Essential roles of ameloblastin in maintaining ameloblast differentiation and enamel formation. Cells Tissues Organs 2005;181:189–195. [PubMed: 16612084]

Fukumoto S, Miner JH, Ida H, Fukumoto E, Yuasa K, Miyazaki H, et al. Laminin alpha5 is required for dental epithelium growth and polarity and the development of tooth bud and shape. J Biol Chem 2006;281:5008–5016. [PubMed: 16365040]

Gibson CW, Yuan ZA, Hall B, Longenecker G, Chen E, Thyagarajan T, et al. Amelogenin-deficient mice display an amelogenesis imperfecta phenotype. J Biol Chem 2001;276:31871–31875. [PubMed: 11406633]

Gibson CW, Kulkarni AB, Wright JT. The use of animal models to explore amelogenin variants in amelogenesis imperfecta. Cells Tissues Organs 2005;181:196–201. [PubMed: 16612085]

Hall A. Rho GTPases and the actin cytoskeleton. Science 1998;279:509–514. [PubMed: 9438836]

Hall A, Nobes CD. Rho GTPases: molecular switches that control the organization and dynamics of the actin cytoskeleton. Philos Trans R Soc Lond B Biol Sci 2000;355:965–970. [PubMed: 11128990]

Hatakeyama J, Sreenath T, Hatakeyama Y, Thyagarajan T, Shum L, Gibson CW, et al. The receptor activator of nuclear factor-kappa B ligand-mediated osteoclastogenic pathway is elevated in amelogenin-null mice. J Biol Chem 2003;278:35743–35748. [PubMed: 12851394]

Hatakeyama J, Philp D, Hatakeyama Y, Haruyama N, Shum L, Aragon MA, et al. Amelogenin-mediated Regulation of Osteoclastogenesis, and Periodontal Cell Proliferation and Migration. J Dent Res 2006;85:144–149. [PubMed: 16434732]

Hu JCC, Hu Y, Smith CE, McKee MD, Wright JT, Yamakoshi Y, et al. Enamel Defects and Ameloblast-specific Expression in *Enam* Knock-out/*lacZ* Knock-in Mice. J Biol Chem 2008;283:10858–10871. [PubMed: 18252720]

Kim JW, Seymen F, Lin BP, Kiziltan B, Gencay K, Simmer JP, et al. ENAM mutations in autosomal-dominant amelogenesis imperfecta. J Dent Res 2005;84:278–282. [PubMed: 15723871]

Krebsbach PH, Lee SK, Matsuki Y, Kozak CA, Yamada KM, Yamada Y. Full-length sequence, localization, and chromosomal mapping of ameloblastin. A novel tooth-specific gene. J Biol Chem 1996;271:4431–4435. [PubMed: 8626794]

Li Y, Decker S, Yuan ZA, Denbesten PK, Aragon MA, Jordan-Sciutto K, et al. Effects of sodium fluoride on the actin cytoskeleton of murine ameloblasts. Arch Oral Biol 2005;50:681–688. [PubMed: 15958199]

Masuya H, Shimizu K, Sezutsu H, Sakuraba Y, Nagano J, Shimizu A, et al. Enamelin (Enam) is essential for amelogenesis: ENU-induced mouse mutants as models for different clinical subtypes of human amelogenesis imperfecta (AI). Hum Mol Genet 2005;14:575–583. [PubMed: 15649948]

Moradian-Oldak J, Goldberg M. Amelogenin supra-molecular assembly in vitro compared with the architecture of the forming enamel matrix. Cells Tissues Organs 2005;181:202–218. [PubMed: 16612086]

Moradian-Oldak J, Du C, Falini G. On the formation of amelogenin microribbons. Eur J Oral Sci 2006;114 (Suppl 1):289–296. [PubMed: 16674701]

Nishikawa S, Kitamura H. Localization of actin during differentiation of the ameloblast, its related epithelial cells and odontoblasts in the rat incisor using NBD-phallacidin. Differentiation 1986;30:237–243. [PubMed: 3699311]

O'Farrell PZ, Goodman HM, O'Farrell PH. High resolution two-dimensional electrophoresis of basic as well as acidic proteins. Cell 1977;12:1133–41. [PubMed: 23215]

Paine ML, Luo W, Zhu DH, Bringas P Jr, Snead ML. Functional domains for amelogenin revealed by compound genetic defects. J Bone Miner Res 2003a;18:466–472. [PubMed: 12619931]

Paine ML, Wang HJ, Luo W, Krebsbach PH, Snead ML. A transgenic animal model resembling amelogenesis imperfecta related to ameloblastin overexpression. J Biol Chem 2003b;278:19447–19452. [PubMed: 12657627]

Peters MF, Ross CA. Isolation of a 40 kDa Huntingtin-associated protein. J Biol Chem 2001;276:3188–3194. [PubMed: 11035034]

Prakash SK, Gibson CW, Wright JT, Boyd C, Cormier T, Sierra R, et al. Tooth enamel defects in mice with a deletion at the Arhgap 6/Amel X locus. Calcif Tissue Int 2005;77:23–29. [PubMed: 16007484]

Simmer JP, Fukae M, Tanabe T, Yamakoshi Y, Uchida T, Xue J, et al. Purification, characterization, and cloning of enamel matrix serine proteinase 1. J Dent Res 1998;77:377–386. [PubMed: 9465170]

Takai Y, Sasaki T, Tanaka K, Nakanishi H. Rho as a regulator of the cytoskeleton. Trends Biochem Sci 1995;20(6):227–231. [PubMed: 7543224]

Li, Yong; Suggs, Cynthia; Wright, J Timothy; Yuan, Zhi-an; Aragon, Melissa; Fong, Hanson, et al. Partial Rescue of the Amelogenin Null Dental Enamel Phenotype. J Biol Chem 2008;283:15056–15062. [PubMed: 18390542]

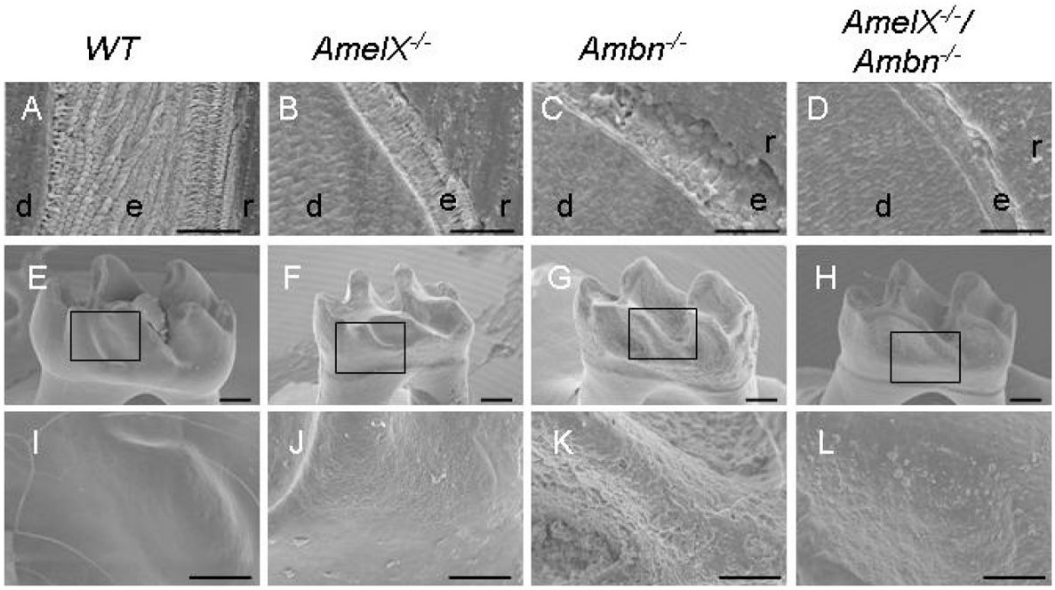

Fig. 1.

Scanning electron microscopy analysis of teeth from *Amel* $X^{-/-}$, *Ambn* $^{-/-}$, *Amel* $X^{-/-}$/ *Ambn* $^{-/-}$, wild-type mice. **A.** (A–D) Incisors from the 6-wk-old mutant and wild-type mice; the enamel (e) in junction with dentin (d) is shown. Note the thin aprismatic structure in *Amel* $X^{-/-}$ mice (B). The enamel-width of *Amel* $X^{-/-}$/*Ambn* $^{-/-}$ (D) mice lacks is markedly reduced as compared with that of the *Ambn* $^{-/-}$ mice (C). **B.** (E–L) molars of the 6-wk-old wild-type and mutant mice; note the small crown size of *Amel* $X^{-/-}$ mice (F) and the double mutant (H). The enamel from *Amel* $X^{-/-}$(F), *Ambn* $^{-/-}$ (G) and *Amel* $X^{-/-}$/*Ambn* $^{-/-}$ (H) appeared abnormal as compared to the wild-type mice (E). (I–L) Teeth from all three mutant mice mimic amelogenesis imperfecta phenotype. *Amel* $X^{-/-}$/*Ambn* $^{-/-}$ enamel appeared less cobbled as compared to *Ambn* $^{-/-}$ enamel Bars in A–D = 50 μm; bar in E–L = 250 μm. (e, enamel; d, dentin; r, resin)

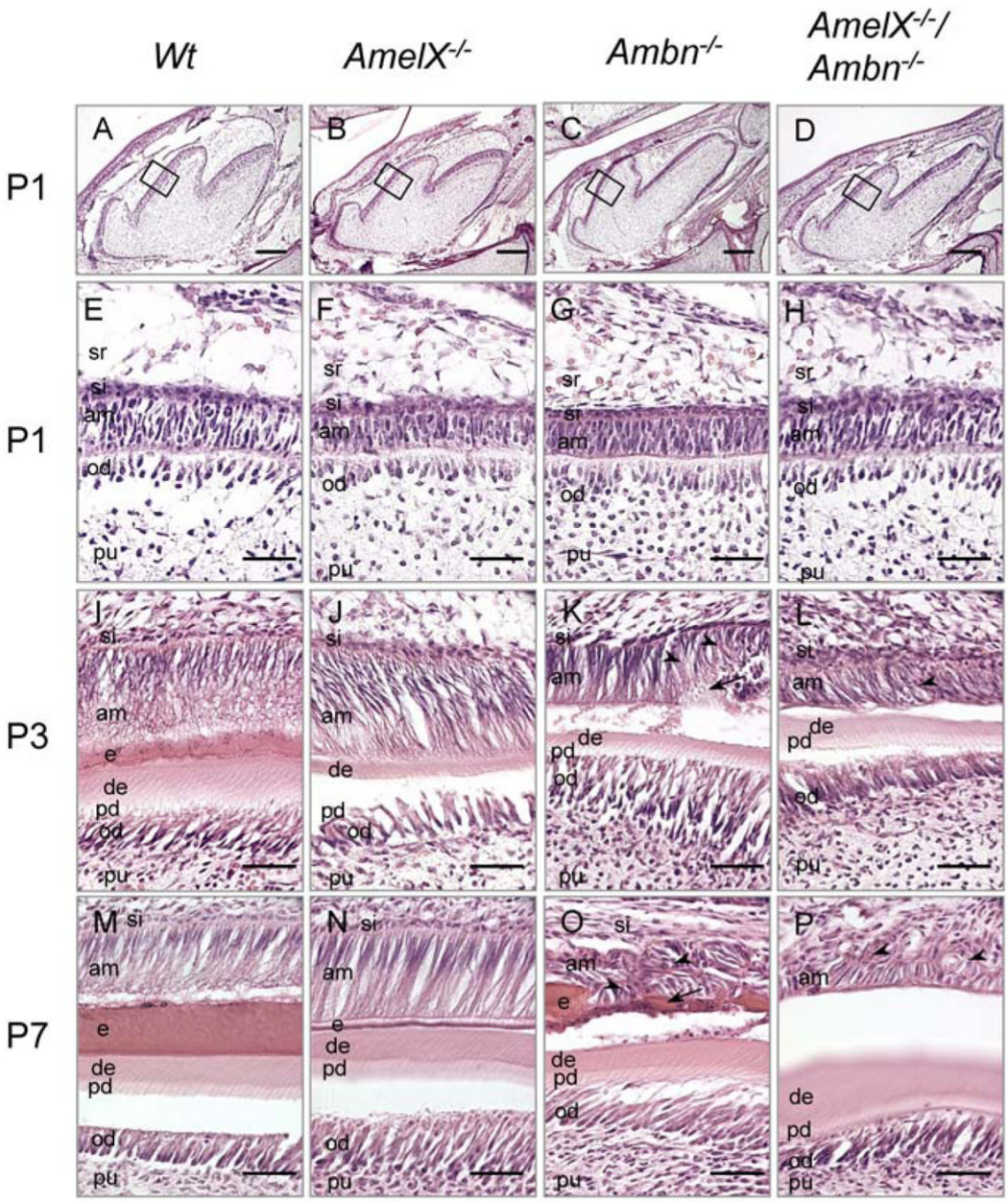

Fig. 2.

Histological analysis of teeth from the wild-type, *Amel X* $^{-/-}$, *Ambn*$^{-/-}$, and *Amel X*$^{-/-}$/*Ambn*$^{-/-}$ mice. Hematoxylin-eosin staining of the sagittal sections of the mandibular first molars of P1 (A–H), P3 (I–L), and P7 (M–P) wild-type and mutant mice: wild-type (A, E, I and M), *Amel X*$^{-/-}$ (B, F, J and N), *Ambn*$^{-/-}$ (C, G, K and O) and *Amel X*$^{-/-}$/*Ambn*$^{-/-}$ mice (D, H, L and P). P3 and P7 *Ambn*$^{-/-}$ ameloblasts display multiple layers containing abnormal calcified structures (Fig. 2K and 2O, arrows). *Amel X*$^{-/-}$/*Ambn*$^{-/-}$ ameloblasts also form multiple layers, however, they do not contain the calcified structures (Fig. 2L and 2P, arrowhead). am, ameloblast; si, stratum intermedium; e, enamel; pd, predentin; de, dentin; od, odontoblast; pu, pulp sr, stellate reticulum). Bars in A–D = 500 μm; bars in E–P = 50 μm.

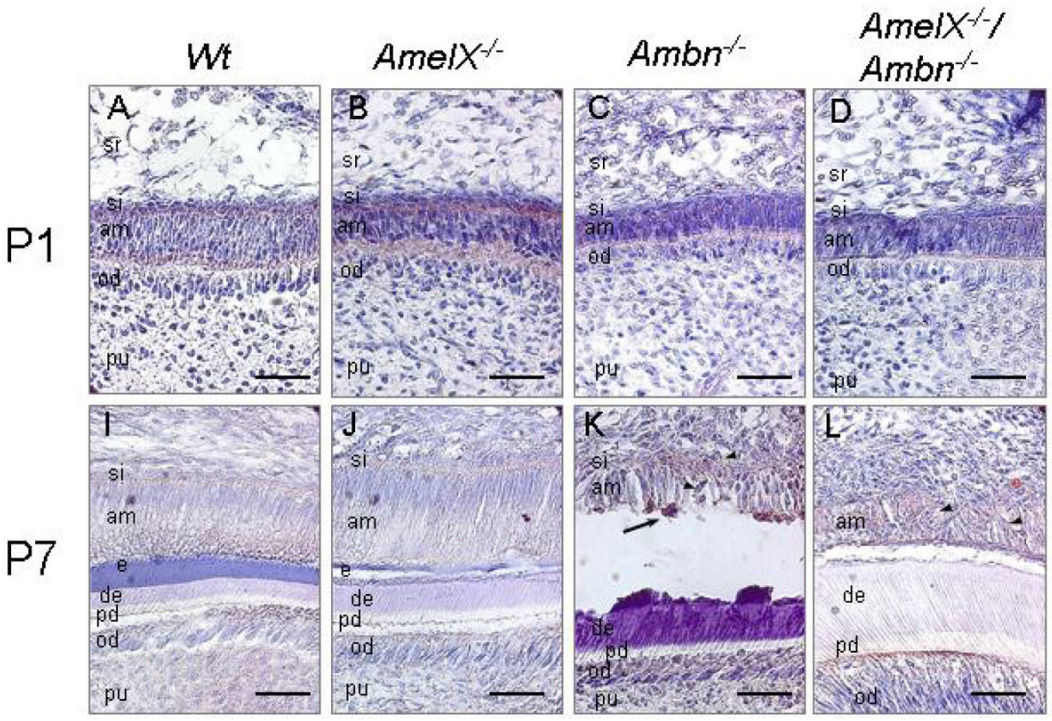

Fig. 3.

RhoGDI expression in the ameloblasts of the wild-type, *Amel X*$^{-/-}$, *Ambn*$^{-/-}$, and *Amel X*$^{-/-}$/*Ambn*$^{-/-}$ mice. Sagittal sections of the incisors from the wild-type (A and E), *Amel X*$^{-/-}$(B and F), *Ambn*$^{-/-}$ (C and G), and *Amel X*$^{-/-}$/*Ambn*$^{-/-}$ mice (D and H) were stained with the RhoGDI antibody as described in Materials and Methods. Note positive staining in the detached ameloblasts of *Ambn*$^{-/-}$ (C and G) and *Amel X*$^{-/-}$/*Ambn*$^{-/-}$ mice (D and H). Bars = 50 μm. am; ameloblast, od; odontoblast, pu; pulp, si, stratum intermedia, e; enamel, d; dentin, pd, predentin